Analytical Biochemistry 509 (2016) 82–88

Contents lists available at ScienceDirect

Analytical Biochemistry

journal homepage: www.elsevier.com/locate/yabio

Subcellular fractionation of human liver reveals limits in global proteomic quantification from isolated fractions

Jacek R. Wiśniewski [a, *], Christine Wegler [b, d], Per Artursson [b, c]

[a] Biochemical Proteomics Group, Department of Proteomics and Signal Transduction, Max Planck Institute of Biochemistry, D-82152 Martinsried, Germany
[b] Department of Pharmacy, Uppsala University, S-751 23 Uppsala, Sweden
[c] Science for Life Laboratory, Uppsala University, S-751 23 Uppsala, Sweden
[d] Cardiovascular and Metabolic Diseases, Innovative Medicines and Early Development Biotech Unit, AstraZeneca, Pepparedsleden 1, Mölndal, S-431 83, Sweden

ARTICLE INFO

Article history:
Received 10 May 2016
Accepted 4 June 2016
Available online 14 June 2016

Keywords:
Human liver
Subcellular fractionation
Absolute quantitative proteomics
Total protein approach
Drug metabolism
Drug transport

ABSTRACT

The liver plays an important role in metabolism and elimination of xenobiotics, including drugs. Determination of concentrations of proteins involved in uptake, distribution, metabolism, and excretion of xenobiotics is required to understand and predict elimination mechanisms in this tissue. In this work, we have fractionated homogenates of snap-frozen human liver by differential centrifugation and performed quantitative mass spectrometry-based proteomic analysis of each fraction. Concentrations of proteins were calculated by the "total protein approach". A total of 4586 proteins were identified by at least five peptides and were quantified in all fractions. We found that the xenobiotics transporters of the canalicular and basolateral membranes were differentially enriched in the subcellular fractions and that phase I and II metabolizing enzymes, the cytochrome P450s and the UDP–glucuronyl transferases, have complex subcellular distributions. These findings show that there is no simple way to scale the data from measurements in arbitrarily selected membrane fractions using a single scaling factor for all the proteins of interest. This study also provides the first absolute quantitative subcellular catalog of human liver proteins obtained from frozen tissue specimens. Our data provide quantitative insights into the subcellular distribution of proteins and can be used as a guide for development of fractionation procedures.

Determination of titers of proteins involved in hepatobiliary elimination and metabolism of drugs and other xenobiotics provides essential information for drug discovery and development. Usually, targeted mass spectrometry (MS) analyses using stable isotope-labeled standards by so-called "targeted proteomics" are used for this purpose. Because targeted mass spectrometry has limitations in sensitivity, concentrations of membrane transporters and drug metabolizing enzymes are generally measured in subcellular fractions such as microsomal pellets and enriched plasma membranes obtained by differential centrifugation or using commercially available kits [1–4]. However, subcellular fractionation is often accompanied by substantial losses of subcellular components, and therefore scaling of protein abundance from subcellular fractions to whole cell or organ abundances has been used [5]. The accuracy of the scaling leans on the assumption that all proteins in the membrane fraction are equally scalable, that is, that a single scaling factor can be used for all of the proteins of interest. Surprisingly, direct evidence of the accuracy of such scaling approaches is missing.

The "total protein approach" (TPA) is an alternative to targeted proteomics [6,7]. This computational approach uses standard and label-free mass spectrometry-based data and is applicable to any biological sample [6]. The method allows profiling of protein abundances expressed in concentrations across tissues and organs [8,9]. Recently, we applied this technology to measure levels of proteins primarily involved in xenobiotics metabolism in human liver, purified hepatocytes, and their membrane preparations [10,11].

In this work, we carried out subcellular fractionation of snap-frozen human liver tissues and applied the label-free technology to measure protein concentrations. Absolute protein content of

Abbreviations used: MS, mass spectrometry; TPA, total protein approach; SDS, sodium dodecyl sulfate; MED–FASP, multiple enzymes for sample digestion–filter-aided sample preparation; WF assay, tryptophan–fluorescence assay; LC, liquid chromatography; MS/MS, tandem mass spectrometry; ER, endoplasmic reticulum; ADME, absorption, distribution, metabolism, and excretion; SLC, solute carrier; ABC, ATP-binding cassette; CYP, cytochrome P450; UGT, UDP–glucuronosyltransferase.

* Corresponding author.
E-mail address: jwisniew@biochem.mpg.de (J.R. Wiśniewski).

http://dx.doi.org/10.1016/j.ab.2016.06.006

individual proteins was calculated by combining the total protein content (determined with our recently introduced protein assay [12]) with the TPA-based protein concentrations. This allowed us to assess the yields for each quantified protein in the homogenate and the subcellular fractions, respectively. We found excellent balance between concentrations in the homogenate and the subcellular fractions combined, indicating good accuracy of the analytical and computational approaches used. Analysis of the quantitative distribution of subcellular marker proteins as well as drug transporters and drug metabolizing enzymes revealed that both plasma membranes and endoplasmic reticulum are heterogeneous to an extent that compromises proper scaling. Based on this observation, we conclude that accurate scaling of protein concentrations measured in arbitrarily selected subcellular fractions to whole tissue values is difficult or even impossible.

Materials and methods

Human liver

Samples of normal human liver tissue were obtained from two donors undergoing surgical resections carried out at the Department of Surgery at Uppsala University Hospital. The resections were immediately snap-frozen in methyl butane on dry ice and ethanol and were stored at −150 °C. All donors gave their informed consent. Ethical approval was granted by the Uppsala Regional Ethics Committee (ethical approvals 2009/028 and 2011/037).

Subcellular fractionation

The frozen pieces of liver (~100 mg) were thawed, cut into small pieces on ice, and suspended in 3 ml of homogenization buffer composed of 0.33 M sucrose, 10 mM $MgCl_2$, and 50 mM Tris–HCl (pH 7.8). The tissue was homogenized at 0 °C in a Teflon–glass Potter S homogenizer at 1200 rpm with 30 down–up cycles. The homogenate (H) was fractionated by successive centrifugation pelleting. Fractions were collected after centrifugation at 1000 *g* for 10 min (fraction A), 2000 *g* for 10 min (fraction B), 5000 *g* for 10 min (fraction C), 10,000 *g* for 10 min (fraction D), and 21,000 *g* for 60 min (fraction E). The remaining supernatant was named cytosol (fraction F).

Protein lysis and proteomic sample preparation

The fractions were lysed in 0.1 M Tris–HCl (pH 8.0) containing 50 mM dithiothreitol (DTT) and 2% sodium dodecyl sulfate (SDS) (w/v) in boiling water for 4 min. After cooling to room temperature, the lysates were clarified by centrifugation at 16,000 *g* for 10 min. The lysates were processed according to the MED–FASP (multiple enzymes for sample digestion–filter-aided sample preparation) protocol using endoproteinase LysC and trypsin [13]. Total protein and total peptide contents were determined using the tryptophan–fluorescence (WF) assay, as described recently [12].

LC–MS/MS and data analysis

Aliquots containing 6-μg peptides were separated on a reverse phase column (50 cm × 75 μm i.d.) packed with 1.8 μm C18 using a 3-h acetonitrile gradient in 0.1% formic acid at a flow rate of 200 nl/min. The liquid chromatography (LC) was coupled to a Q Exactive HF mass spectrometer (Thermo Fisher Scientific, Germany) via a nanoelectrospray source (Proxeon Biosystems, now Thermo Fisher Scientific). The mass spectrometer operated in data-dependent mode with survey scans acquired at a resolution of 60,000 in a range of 300–1650 *m/z*. Up to the top 15 most abundant isotope patterns with charge ≥ +2 from the survey scan were selected with an isolation window of 1.4 *m/z* and fragmented by HCD (higher energy collisional dissociation) with normalized collision energies of 25. The maximum ion injection times for the survey scan and the tandem mass spectrometry (MS/MS) scans were 20 and 60 ms, and the ion target values were 3×10^6 and 1×10^5, respectively. The dynamic exclusion was 30 s.

Data analysis

The MS data were analyzed using MaxQuant software (version 1.5.3.14). Proteins were identified by searching MS and MS/MS data of peptides against a decoy version of UniProtKB (August 2015) containing 50,807 sequences. The search was performed with a fragment ion mass tolerance of 0.5 Da and a parent ion tolerance of 20 ppm. The protein and peptide false discovery rates were set to 1%. Protein abundances were calculated from the spectral raw intensities using the TPA [6,7] with the relationships:

$$Total\ \ protein(i) = \frac{MS-signal(i)}{Total\ \ MS-signal}$$

$$Protein\ \ concentration(i) = \frac{MS-signal(i)}{Total\ \ MS-signal \times MW(i)} \left[\frac{mol}{g\ \ total\ \ protein}\right].$$

Protein yields in the subcellular fractions were assessed using the biochemically (*bioch.*) measured total protein concentration by the WF assay, and the "virtual" protein concentrations were calculated using the TPA:

$$Protein\ \ yield(i) = Protein\ \ concentration\ (i) \times \left[\frac{\sum bioch.\ total\ \ protein\ \ in\ \ fractions}{bioch.\ total\ \ protein\ \ in\ \ homogenate}\right].$$

Calculations were performed in Excel (Microsoft). Statistical analyses were carried out in SigmaPlot12 (SigmaPlot).

Results

Fractionation of human liver and identification of proteins

The human liver samples originated from two donors and were processed separately. Pieces of tissue (100 mg) were homogenized and fractionated by differential pelleting into five fractions, A to E, where fraction A was expected to be dominated by nuclei and fractions B, C, D, and E were expected to be dominated by mitochondria, membrane fractions from Golgi body, endoplasmic reticulum (ER), and plasma membranes, respectively. The remaining supernatant was named cytosol (fraction F) (Fig. 1A). Aliquots of the homogenate and the entire fractions A to F were lysed in SDS-

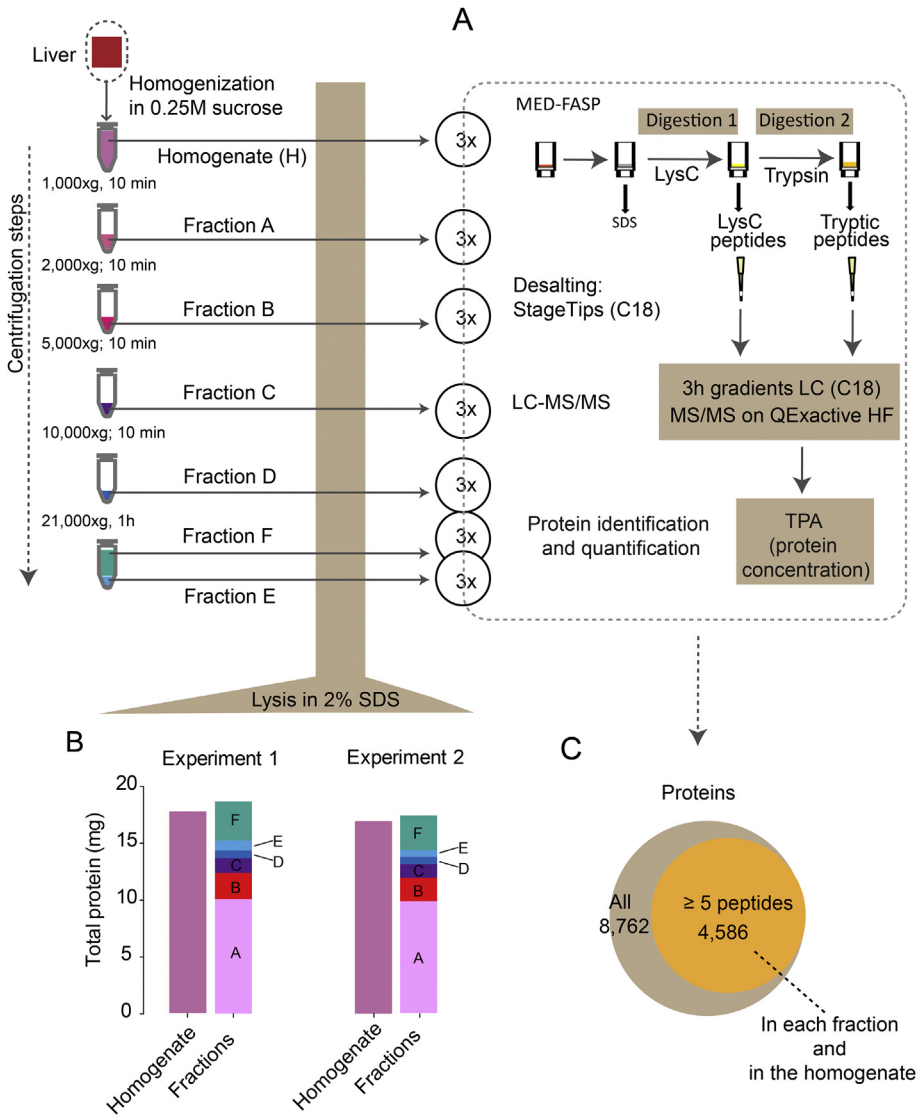

Fig.1. Tissue fractionation and proteomic analysis workflows applied to human liver samples. Frozen human liver samples were homogenized in buffered 0.25 M sucrose and the homogenate (A) was fractionated by differential pelleting into six fractions, A to F. Triplicate aliquots of each subcellular fraction were lysed in 2% SDS and processed by the MED–FASP procedure using endoproteinase LysC and trypsin. The released peptides were analyzed by LC–MS/MS, and the spectra were searched using MaxQuant software. Concentrations of individual proteins were assessed by the TPA. (B) Balance of the total protein content in the homogenates and centrifugal fractions, A to F. (C) Protein identifications and quantification. In total, 8762 proteins were identified, of which 4586 were identified with at least five peptides and were found in each fraction.

Table 1
Distribution and recoveries of total protein.

Fraction	Centrifugal conditions	Experiment 1 total protein (mg)	Experiment 2 total protein (mg)	Average total protein (mg)	Average total protein (%)
H	Homogenate	16.3	16.6	16.45	100.0
A	1000 *g*, 10 min	10.1	9.8	9.95	60.5
B	2000 *g*, 10 min	2.3	2.2	2.25	13.7
C	5000 *g*, 10 min	1.3	1.3	1.3	7.9
D	10,000 *g*, 10 min	0.66	0.48	0.57	3.5
E	21,000 *g*, 60 min	0.88	0.52	0.70	4.3
F	Cytosol	3.2	3.1	3.15	19.1
Sum fractions A–F (mg)		18.44	17.4	17.92	
Yield (%)[a]		113	104	108	

[a] Yield = {Σ(fractions A–F)/homogenate}*100%.

containing buffer. The sum of the total protein contents in the generated fractions (fractions A–F in Fig. 1A) was close to 100% of the total protein content in the homogenate, indicating high yield of the preparative procedures (Fig. 1B and Table 1). Fraction A was most prominent, comprising approximately 50% of total protein of the homogenate. In contrast, the pellet collected at 21,000 *g* (fraction E) contained only 3–5% of the total protein (Table 1).

The MED–FASP procedure allowed conversion of the proteins

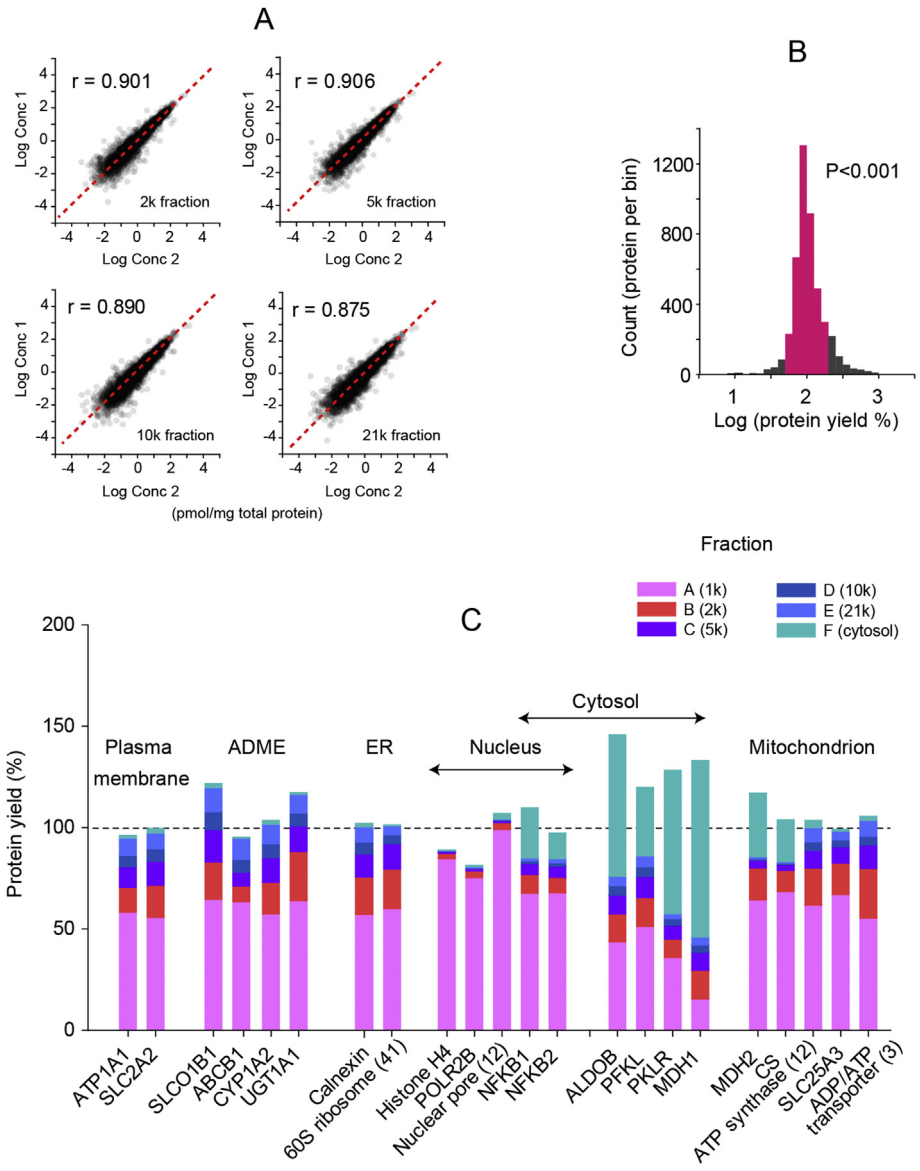

Fig.2. Quantitative analysis of the data across the fractions. (A) Comparison of protein concentrations measured in 2 k, 5 k, 10 k, and 20 k fractions in two independent experiments (1 and 2). P, Pearson correlation coefficient. (B) Yields of 4586 quantified proteins. There is a statistically significant difference between the median of the group and the hypothesized population median at $P < 0.001$. The highlighted area indicates 95% of the yield values. (C) Yields and partition of the selected proteins in the subcellular fractions relative to the homogenate. For 60 S ribosome, nuclear pore, ATP synthase and ADP/ATP transporter average values of their subunits are shown. The numbers of subunits are given in parentheses.

into peptides at a yield of 70–90% (not shown). The samples were analyzed by LC–MS/MS in triplicates (Fig. 1A), and the analysis led to the identification of 111,000 peptides representing 8762 proteins (Fig. 1C; see also Supplemental Table 1 in the online supplementary material). Of these, 4586 proteins were identified by at least five peptides and were found in each subcellular fraction and in the homogenate. Only this subset of identified protein was subject to further quantitative analyses by the TPA providing absolute values (i.e., protein fractions per total protein or specific protein concentration in mol per mass of total protein) (Supplemental Table 1). These values allowed yield calculations of individual proteins across the fractions compared with the homogenate.

Quantitative analysis of protein fractions

Comparison of the MS-based protein concentration data showed a good correlation between both experiments (Fig. 2A). Combining the values of total protein per fraction (Table 1) with the protein concentrations (Supplemental Table 1) enabled calculation of balances between fractions A to F and the homogenate for the quantified proteins. Fully 95% of these values were within the interval of 50–200% (highlighted area in Fig. 2B). A one-sample *t*-test revealed a statistically significant difference between the median of the yield values and the hypothesized yields population median ($P < 0.001$), indicating on average excellent recovery of the majority of the proteins. Fig. 2C shows examples of the distribution of protein contents across fractions compared with the homogenate.

Proteins specific to plasma membrane such as subunit A of (Na^+/K^+)ATPase (ATP1A1) and the glucose transporter Glut2 (SLC2A2) were distributed across all fractions, with their largest portion being in the "nuclear pellet" (fraction A) (Fig. 2C). Similar distribution of the protein contents was also observed for membrane proteins involved in drug transport and degradation processes (ADME [absorption, distribution, metabolism, and excretion]

proteins) and proteins of the endoplasmic reticulum. Proteins with constitutive nuclear location, such as histone H4, RNA–polymerase II, and nuclear pore complex subunits, were present in at least 95% of fraction A, whereas soluble cytoplasmic proteins were present mainly in the cytosolic fraction (fraction F). The transcription factor NFκB (nuclear factor kappa B) that is known to shuttle between the cytoplasm and nucleus was identified at 60% in nucleus and 30% in cytoplasm. Unexpectedly, considerable amounts of 20–30% of the total content of non-membrane proteins of the mitochondrial matrix, such as citrate synthase and malate dehydrogenase 2, were found in the cytosol fraction. This presumably reflects leakage from mitochondria due to tissue freezing.

Analysis of the quantitative distribution of the proteins across the fractions revealed that the 21,000 *g* supernatant (fraction F) contained negligible low amounts of membrane proteins from plasma membrane, ER, and mitochondria (Fig. 2C). This indicates that using medium-speed (21,000 *g*) centrifugation is sufficient to obtain complete microsomal fraction and that ultracentrifugation at 100,000 *g* would not be required. Notably, a similar observation was made by Abas and Luschnig for plant microsomes [14].

Subcellular distribution of membrane proteins involved in xenobiotics elimination

The hepatobiliary elimination of drugs and other xenobiotics consists of four major stages. It commences by basolateral uptake, involves two phases of metabolism, and terminates by biliary (canalicular) or apical efflux of the metabolites (Fig. 3A). Membrane transport proteins of the solute carrier (SLC) family facilitate the hepatic uptake of drugs, whereas excretion into the bile and blood is mainly carried out by transporters of the ATP-binding cassette (ABC) family. Cytochrome P450s (CYPs) and UDP–glucuronosyltransferases (UGTs) are key enzymes of the phase I and phase II metabolism of xenobiotics. To analyze the distribution of these proteins across the subcellular fractions, we calculated the enrichment in fractions E and F, respectively, relative to the "post-nuclear" fraction C. We observed that each group of the proteins important for the xenobiotic clearance clustered together in different fractions, revealing specific enrichment profiles (Fig. 3B–E). The transporters showed a continuous enrichment with the increased centrifugal speed used for fraction collection (Fig. 3B and C). In contrast, the enzymes did not follow this trend (Fig. 3D and E). Notably, proteins located in the basolateral and canalicular plasma membranes, respectively, were not distributed equally (Fig. 3B and C). (Na^+/K^+)ATPase that is abundant in the basolateral membrane had an enrichment profile similar to that of the basolaterally located transporters, supporting the notion that this protein can be used as a marker for sinusoidal plasma membrane fractions [4] (cf. Fig. 3F and B). The efflux transporter ABCC3, which is also located in the basolateral plasma membrane, showed an enrichment profile similar to that of the basolateral uptake transporters. Because the basolateral transporters were also found in the other fractions, we compared the protein concentrations of the transporters with the (Na^+/K^+)ATPase across all fractions and the homogenate (Fig. 4). All transporters of the basolateral membrane showed a good correlation with the ATPase. In contrast, the canalicular transporters ABCC2 and ABCG5 did not correlate with the ATPase titers.

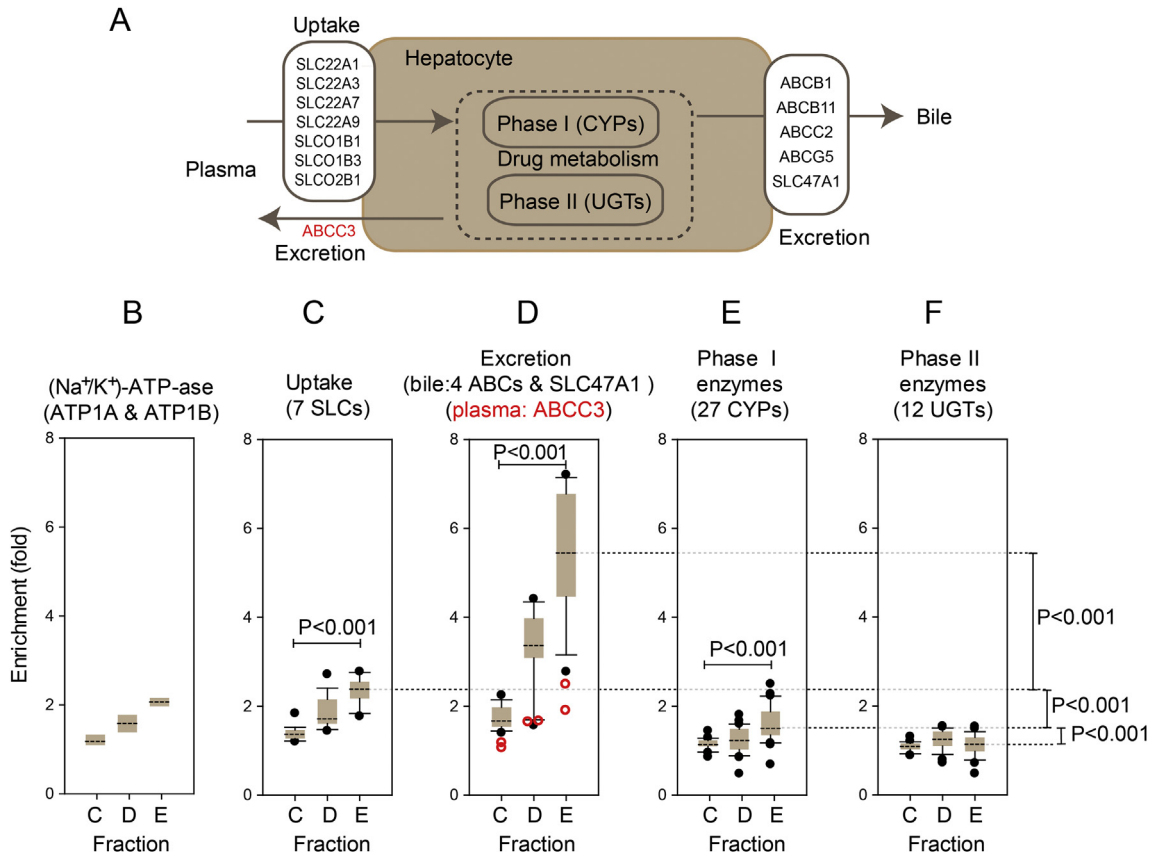

Fig.3. Group-specific enrichment profiles of the key proteins involved in drug transport and metabolism. (A) Scheme of the hepatobiliary elimination of drugs and other xenobiotics by hepatocytes. (B–F) Partition of the (Na^+/K^+)ATPase (B) and proteins involved in basolateral uptake (C), biliary/sinusoidal efflux (D), and phase I and phase II metabolism (E and F, respectively). Protein enrichment values were calculated against concentrations in the 2 k fraction.

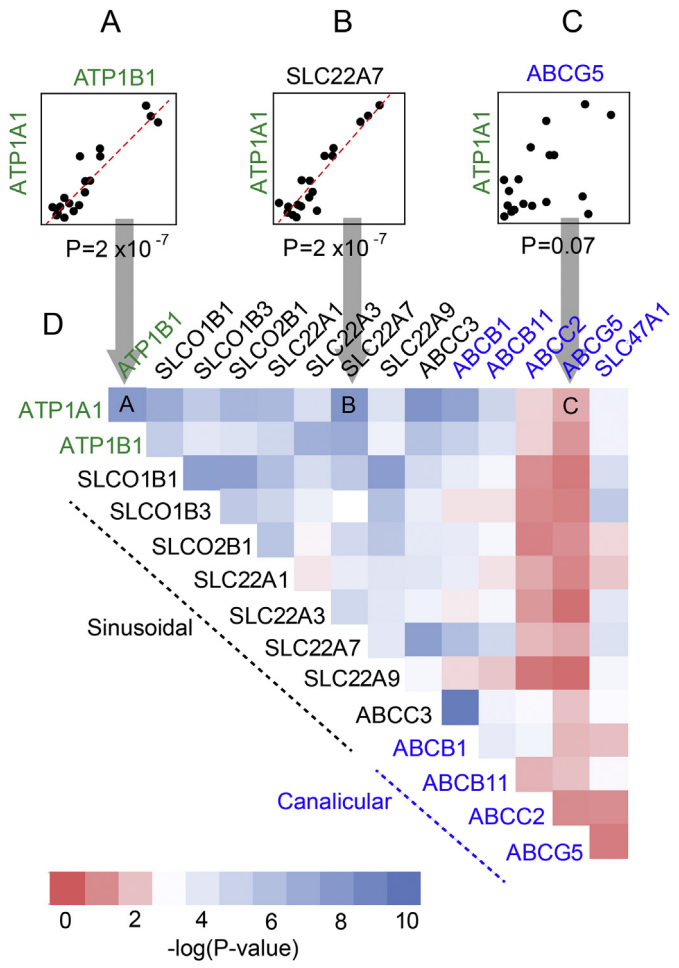

Fig.4. Correlation of the membrane transporter and (Na^+/K^+)ATPase concentrations across the fractions (A–E) and homogenate. (A–C) Correlation of protein concentrations of ATP1B1 (subunit B of (Na^+/K^+)ATPase), SLC22A7, and ABCG5 with ATP1A1 (subunit A of (Na^+/K^+)ATPase). Each data point reflects a single measurement. (D) Heatmap with *P*-values of the Spearman rank correlations between the transporters of the sinusoidal (black), canalicular (blue), and plasma membrane (Na^+/K^+)ATPase (green). Correlation plots shown in panels A, B, and C are a part of the heatmap.

Discussion

Subcellular fractionation of animal liver tissue has been the subject of many studies. In contrast, reports on fractionation of human liver tissue are scarce [15,16]. This presumably reflects limited availability of fresh human tissue for research as well as difficulties in subcellular fractionation of cryopreserved tissue. A study on subcellular fractionation comparing fresh and frozen murine liver tissues revealed significantly decreased yields after fractionation of the frozen tissue [17]. This was in agreement with extensive damage of mitochondria and nuclei in the subcellular fractions from the frozen material, as observed by electron microscopy. Both factors negatively influenced the separation of organelles.

Our analyses are in line with these findings. We observed that, with the exception of nuclei, all organelle-specific proteins were widely distributed among the different pellet fractions. Based on the total protein measurements, more than 50% of the subcellular material was recovered in the first fraction collected at 1000 *g* (fraction A). This fraction is often considered as nuclear, but in hepatocytes, the major cell fraction in liver, nuclei account for 5–7% of the cell volume [18] and approximately 10% of the total cell protein [10]. Thus, our results indicate that approximately 90% of this fraction contains cell material that is inert to standard homogenization. Inversely, fraction E comprised only 3–5% of the total protein, which is 2–3 times less than what had been isolated from *fresh* human liver tissue [19]. In addition, we also found a portion of mitochondria-specific soluble enzymes in the cytosolic fraction. This seems to be an indication of *freezing*-associated damage of mitochondria and subsequent leakage of soluble components from the matrix. Apart from the effect of the structural damage on the fractionation procedure, two other factors may contribute to suboptimal distribution of the mitochondrial proteins: the occurrence of large amounts of glycogen and blood in liver tissue.

Human liver accumulates large amounts of glycogen, which can constitute up to 10% (w/w) of the tissue. The effects of this natural polymer on subcellular fractionation have already been recognized in the past, and therefore animals are routinely starved before experiments [20]. Because human liver samples may contain significant amounts of glycogen, a possible effect of this polymer on subcellular fractionation cannot be ruled out. However, the glycogen levels were most likely lowered in our samples due to standard fasting regimes prior to surgery. The second factor, the occurrence of blood, that potentially affects the subcellular fractionation can, at least, be partially eliminated by washing of fresh liver cut into small fragments. Coagulation of blood can also be a problem, which is prevented by adding ethylenediaminetetraacetic acid (EDTA) to the homogenization buffer. In the frozen tissue, blood is coagulated and the clots may generate aggregates during the tissue homogenization. In line with this, we found one of the most abundant blood proteins, hemoglobin, in all subcellular fractions at concentrations similar to or exceeding that in the homogenate (see Supplemental Table 1 in supplementary material).

Furthermore, data generated from targeted spike-in analyses are often considered as accurate. However, the results can be heavily biased by partial digestion [21] of the samples and the fact that single or only few peptides are used for the quantification. This seems to be one of the reasons for large differences in concentrations of the ADME proteins in liver, reported by several groups [22,23]. In contrast, in global proteomic analysis using the TPA, protein abundances are calculated on the basis of spectral MS^1 intensities of many peptides. For example, in this study the concentrations of the 4586 proteins were calculated on the basis of, on average, 20 peptides per protein against 111,000 peptides in the whole dataset. In this context, we also should refer to our recent study showing a comparison of the TPA and a spike in the prEST (protein epitope signature tag) approach [24] that revealed an average deviation of only 1.5-fold in the protein titers calculated by both methods [6].

Traditionally, subcellular fractionation of tissue was accompanied by determination of total protein content and enzymatic activities across all fractions and the homogenate. This information allowed calculation of yields of the procedure and gave indications of the content and purity of the isolated subcellular fractions. Over time, many of the laborious biochemical assays were replaced by Western blot analyses. At best, both biochemical and Western blot analyses enable insights into the subcellular distribution of a limited number of proteins. In contrast, large-scale proteomics can provide a system-wide picture based on quantitative analysis of all fractions obtained. The TPA allows quantitative analyses of thousands of proteins, assessing their content and concentrations across all analyzed fractions. Combining the TPA data with biochemical total protein measurements enables calculation of the protein contents per individual fraction. This information provides quantitative insights into the subcellular distribution of proteins and can be used as a guide for development of fractionation procedures.

Our analyses clearly demonstrate that upscaling of the quantitative data generated for single subcellular fractions is not possible without knowledge of the actual subcellular location and enrichment factors. Furthermore, our analysis indicates that membrane proteins involved in different phases of xenobiotics elimination are heterogeneously distributed in the liver cells, and therefore their abundance in liver cannot be correctly assessed from analysis of single fractions such as the microsomal fraction.

Conclusions

We demonstrate that subcellular fractionation of frozen human tissue is a difficult task that does not result in fractions identical to those that can be achieved from fresh animal tissue. We combined total protein assays with values of virtually quantified proteins using the TPA in order to calculate a quantitative yield balance between the summed subcellular fractions and the homogenate. Our data show that measuring protein levels in single subcellular fractions does not allow simple upscaling of data to whole tissue. In contrast, this can be achieved by label-free in-depth proteomics analysis of whole tissue lysate and the computational tool, the TPA. To our knowledge, this study also provides the first absolute quantitative subcellular catalog of human liver proteins obtained from frozen tissue specimens.

Acknowledgments

The authors are grateful to Matthias Mann for continuous support and Katharina Zettl for technical assistance. We also thank Agneta Norén and the surgery team at Uppsala University Hospital for contributing in the clinical sampling. This work was supported by the Max Planck Society for the Advancement of Science by the German Research Foundation (DFG/Gottfried Wilhelm Leibniz Prize), and the Swedish Research Council (grant 2822).

Appendix A. Supplementary data

Supplementary data related to this article can be found at http://dx.doi.org/10.1016/j.ab.2016.06.006.

References

[1] B. Prasad, R. Evers, A. Gupta, C.E. Hop, L. Salphati, S. Shukla, S.V. Ambudkar, J.D. Unadkat, Interindividual variability in hepatic organic anion-transporting polypeptides and P-glycoprotein (ABCB1) protein expression: quantification by liquid chromatography tandem mass spectroscopy and influence of genotype, age, and sex, Drug Metab. Dispos. 42 (2014) 78–88.
[2] T.G. Tucker, A.M. Milne, S. Fournel-Gigleux, K.S. Fenner, M.W. Coughtrie, Absolute immunoquantification of the expression of ABC transporters P-glycoprotein, breast cancer resistance protein, and multidrug resistance-associated protein 2 in human liver and duodenum, Biochem. Pharmacol. 83 (2012) 279–285.
[3] O. Schaefer, S. Ohtsuki, H. Kawakami, T. Inoue, S. Liehner, A. Saito, A. Sakamoto, N. Ishiguro, T. Matsumaru, T. Terasaki, T. Ebner, Absolute quantification and differential expression of drug transporters, cytochrome P450 enzymes, and UDP–glucuronosyltransferases in cultured primary human hepatocytes, Drug Metab. Dispos. 40 (2012) 93–103.
[4] V. Kumar, B. Prasad, G. Patilea, A. Gupta, L. Salphati, R. Evers, C.E. Hop, J.D. Unadkat, Quantitative transporter proteomics by liquid chromatography with tandem mass spectrometry: addressing methodologic issues of plasma membrane isolation and expression–activity relationship, Drug Metab. Dispos. 43 (2015) 284–288.
[5] M.D. Harwood, M.R. Russell, S. Neuhoff, G. Warhurst, A. Rostami-Hodjegan, Lost in centrifugation: accounting for transporter protein losses in quantitative targeted absolute proteomics, Drug Metab. Dispos. 42 (2014) 1766–1772.
[6] J.R. Wisniewski, M.Y. Hein, J. Cox, M. Mann, A "proteomic ruler" for protein copy number and concentration estimation without spike-in standards, Mol. Cell. Proteomics 13 (2014) 3497–3506.
[7] J.R. Wisniewski, D. Rakus, Multi-enzyme digestion FASP and the "total protein approach"-based absolute quantification of the *Escherichia coli* proteome, J. Proteomics 109 (2014) 322–331.
[8] J.R. Wisniewski, A. Gizak, D. Rakus, Integrating proteomics and enzyme kinetics reveals tissue-specific types of the glycolytic and gluconeogenic pathways, J. Proteome Res. 14 (2015) 3263–3273.
[9] J.R. Wisniewski, H. Koepsell, A. Gizak, D. Rakus, Absolute protein quantification allows differentiation of cell-specific metabolic routes and functions, Proteomics 15 (2015) 1316–1325.
[10] J.R. Wisniewski, A. Vildhede, A. Noren, P. Artursson, In-depth quantitative analysis and comparison of the human hepatocyte and hepatoma cell line HepG2 proteomes, J. Proteomics 136 (2016) 234–247.
[11] A. Vildhede, J.R. Wisniewski, A. Noren, M. Karlgren, P. Artursson, Comparative proteomic analysis of human liver tissue and isolated hepatocytes with a focus on proteins determining drug exposure, J. Proteome Res. 14 (2015) 3305–3314.
[12] J.R. Wisniewski, F.Z. Gaugaz, Fast and sensitive total protein and peptide assays for proteomic analysis, Anal. Chem. 87 (2015) 4110–4116.
[13] J.R. Wisniewski, M. Mann, Consecutive proteolytic digestion in an enzyme reactor increases depth of proteomic and phosphoproteomic analysis, Anal. Chem. 84 (2012) 2631–2637.
[14] L. Abas, C. Luschnig, Maximum yields of microsomal-type membranes from small amounts of plant material without requiring ultracentrifugation, Anal. Biochem. 401 (2010) 217–227.
[15] P. Bjorntorp, S. Bjorkerud, T. Schersten, Subcellular fractionation of human liver, Biochim. Biophys. Acta 111 (1965) 375–383.
[16] T.J. Peters, C.A. Seymour, Analytical subcellular fractionation of needle-biopsy specimens from human liver, Biochem. J. 174 (1978) 435–446.
[17] Y. Song, Y. Hao, A. Sun, T. Li, W. Li, L. Guo, Y. Yan, C. Geng, N. Chen, F. Zhong, H. Wei, Y. Jiang, F. He, Sample preparation project for the subcellular proteome of mouse liver, Proteomics 6 (2006) 5269–5277.
[18] E.R. Weibel, W. Staubli, H.R. Gnagi, F.A. Hess, Correlated morphometric and biochemical studies on the liver cell: I. Morphometric model, stereologic methods, and normal morphometric data for rat liver, J. Cell Biol. 42 (1969) 68–91.
[19] G.E. Palade, P. Siekevitz, Liver microsomes: an integrated morphological and biochemical study, J. Biophys. Biochem. Cytol. 2 (1956) 171–200.
[20] S. Fleischer, M. Kervina, Subcellular fractionation of rat liver, Methods Enzymol. 31 (1974) 6–41.
[21] T. Glatter, C. Ludwig, E. Ahrne, R. Aebersold, A.J. Heck, A. Schmidt, Large-scale quantitative assessment of different in-solution protein digestion protocols reveals superior cleavage efficiency of tandem Lys-C/trypsin proteolysis over trypsin digestion, J. Proteome Res. 11 (2012) 5145–5156.
[22] B. Achour, J. Barber, A. Rostami-Hodjegan, Expression of hepatic drug-metabolizing cytochrome P450 enzymes and their intercorrelations: a meta-analysis, Drug Metab. Dispos. 42 (2014) 1349–1356.
[23] B. Achour, A. Rostami-Hodjegan, J. Barber, Protein expression of various hepatic uridine 5′-diphosphate glucuronosyltransferase (UGT) enzymes and their inter-correlations: a meta-analysis, Biopharm. Drug Dispos. 35 (2014) 353–361.
[24] M. Zeiler, M. Moser, M. Mann, Copy number analysis of the murine platelet proteome spanning the complete abundance range, Mol. Cell. Proteomics 13 (2014) 3435–3445.